
Physics-aware Spatiotemporal Modules with Auxiliary Tasks for Meta-Learning

Sungyong Seo*, Chuizheng Meng*, Sirisha Rambhatla, Yan Liu
Department of Computer Science
University of Southern California
{sungyons, chuizhem, sirishar, yanliu.cs}@usc.edu

Abstract

Modeling the dynamics of real-world physical systems is critical for spatiotemporal prediction tasks, but challenging when data is limited. The scarcity of real-world data and the difficulty in reproducing the data distribution hinder directly applying meta-learning techniques. Although the knowledge of governing partial differential equations (PDEs) of the data can be helpful for the fast adaptation to few observations, it is difficult to generalize to different or unknown dynamics. In this paper, we propose a framework, physics-aware modular meta-learning with auxiliary tasks (PiMetaL) whose spatial modules incorporate PDE-independent knowledge and temporal modules are rapidly adaptable to the limited data, respectively. The framework does not require the exact form of governing equations to model the observed spatiotemporal data. Furthermore, it mitigates the need for a large number of real-world tasks for meta-learning by leveraging simulated data. We apply the proposed framework to both synthetic and real-world spatiotemporal prediction tasks and demonstrate its superior performance with limited observations.

1 Introduction

Deep learning has recently shown promise to play a major role in devising new solutions to applications with natural phenomena, such as climate change [1, 2], ocean dynamics [3], air quality [4, 5, 6], and so on. Deep learning techniques inherently require a large amount of data for effective representation learning, so their performance is significantly degraded when there are only a limited number of observations. However, in many tasks in physical world we only have access to a limited amount of data. One example is air quality monitoring [7], in which the sensors are irregularly distributed over the space – many sensors are located in urban areas whereas there are very few sensors in vast rural areas. Another example is extreme weather modeling and forecasting, i.e., temporally short events (e.g., tropical cyclones [8]) without sufficient observations over time. Moreover, inevitable missing values from sensors [9, 10] further reduce the number of operating sensors and shorten the length of fully-observed sequences. Thus, achieving robust performance by quickly learning from a few spatiotemporal observations remains an essential but challenging problem.

Several approaches have been developed to address this challenge by utilizing prior knowledge or previous experience, e.g. meta-learning [11, 12, 13, 14], transfer learning [15], domain adaptation [16, 17], and continual learning [18]. Among them, meta-learning algorithms, which extract common knowledge across multiple *tasks* (meta-train tasks) and reuse it for unseen tasks (meta-test tasks), have emerged as one of the most effective solution as they provide reusable representations and rapid learning algorithm [19]. However, we are confronted with a series of challenges when we apply meta-learning to the real-world spatiotemporal observations governed by known/unknown physics equations. First, it is not easy to find a set of prior datasets which provide shareable

*Equally contributed.

latent representations needed to understand targeted natural phenomena. For instance, while image-related tasks (detection [20] or visual-question-answering tasks [21, 22]) can take advantage of an image-feature extractor that is pre-trained by a large set of images [23] and well-designed architecture [24, 25, 26], there is no such large data corpus that is widely applicable for natural phenomena. Second, unlike computer vision or natural language processing tasks where a common object (images or words) is clearly defined, it is not straightforward to find analogous objects in the spatiotemporal data. Finally, while a governing equation on particular observations can be helpful for an adaptation of a model on few samples, the exact equations behind natural phenomena are usually unknown, leading to the difficulty in reproducing the same real-world data distribution via simulation. For example, there have been some works [27, 28, 29] addressing the data scarcity issue via explicitly incorporating PDEs as neural network layers when modeling spatiotemporal dynamics. While it shows improved data efficiency in modeling data governed by dynamics with known explicit forms, it is hard to generalize for modeling different or unknown dynamics, which is ubiquitous in real-world scenario.

In many PDEs in physics, a time derivative of a physical quantity is a function of spatial derivatives. For example, the convection-diffusion (transportation) and the Navier-Stokes equations (motion of viscous fluid) are:

$$\begin{aligned} \partial u / \partial t &= \nabla \cdot (D \nabla u) - \nabla \cdot (\mathbf{v}u) + R, && \text{(Convection-Diffusion eqn.)} \\ \partial \mathbf{u} / \partial t &= -(\mathbf{u} \cdot \nabla) \mathbf{u} + \nu \nabla^2 \mathbf{u} - \nabla \omega + \mathbf{g}. && \text{(Incompressible Navier-Stokes eqn.)} \end{aligned}$$

where the scalar u and vector field \mathbf{u} are the variables of interest (e.g., temperature, flow velocity, etc.). Since the spatial derivatives such as ∇ , $\nabla \cdot$, and ∇^2 are commonly used in different PDEs, we define spatial derivative modules as PDE-independent modules and provide auxiliary tasks to regularize the modules to approximate the spatial derivatives. Then, another PDE-specific module is combined with spatial modules to learn the relation between spatial and time derivatives. This approach can effectively leverage a large amount of simulated data to train the spatial modules as the modules are PDE-independent and thus mitigating the need for a large amount of real-world tasks to extract shareable features. In addition, since the spatial modules are universally used in physics equations and explicit forms of equations are not required for training the modules, the modular method can conveniently integrate meta-learning for natural phenomena. Based on the modularized PDEs, we introduce a novel approach that marries physics knowledge in spatiotemporal prediction tasks with meta-learning by providing shareable modules across spatiotemporal observations in the real-world.

Our contributions are summarized below:

- **Modularized PDEs with auxiliary tasks:** Inspired by forms of PDEs in physics, we decompose PDEs into shareable (spatial) and adaptation (temporal) parts. The shareable modules are PDE-independent and specified by corresponding auxiliary tasks.
- **Physics-aware modular meta-learning:** We provide a framework for physics-aware modular meta-learning, which consists of PDE-independent/-specific modules. The framework is flexible to be applied to the modeling of different or unknown dynamics.
- **Synthetic data for shareable modules:** We extract shareable parameters in the spatial modules from simulated data, which can be generated from different distributions easily.

2 Motivation

In this section, we describe how the physics equations are decomposable into modules and how the modular meta-learning approach tackles the task when the data are limited.

2.1 Modularizable partial differential equations in physics

It is common that partial differential equations are used to describe many quantities in the real-world. Specifically, a quantity associated with natural phenomena or physics such as temperature, fluid density, and object state is given as a function of spatial and temporal input, $u = u(\mathbf{x}, t)$, where u is the target quantity and is governed by some PDE. A PDE formulates how the quantity is varying along the two axes: space and time.

For $u(\mathbf{x}, t)$ where $\mathbf{x} = (x, y)$ coordinates in 2D space, a general form of PDEs is

$$f\left(x, y, t; u, \frac{\partial u}{\partial x}, \frac{\partial u}{\partial y}, \frac{\partial^2 u}{\partial x^2}, \frac{\partial^2 u}{\partial y^2}, \dots; \frac{\partial u}{\partial t}, \frac{\partial^2 u}{\partial t^2}, \dots\right) = 0. \quad (1)$$

The form can be digested for many physics-associated quantities [30, 31]:

$$\partial u / \partial t = F(u_x, u_y, u_{xx}, u_{yy}, \dots), \quad (2)$$

where the right-hand side of Eq. 2 denotes a function of spatial derivatives. As the time derivative can be seen as a Euler discretization [32], it is notable that the next state is a function of the current state and spatial derivatives. Thus, for physics-associated quantities, knowing spatial derivatives at time t is a key step for spatiotemporal prediction at time $t + 1$.

2.2 Spatial derivative modules: PDE-independent modules

Finite difference method (FDM) is widely used to discretize a d -order derivative as a linear combination of function values on a n -point stencil.

$$\frac{\partial^d u}{\partial x^d} \approx \sum_{i=1}^n \alpha_i u(x_i), \quad (3)$$

where $n > d$. According to FDM, it is independent for a form of PDE to compute spatial derivatives, which are input components of $F(\cdot)$ in Eq. 2. Thus, we can modularize spatial derivatives as PDE-independent modules. The modules that can be learnable as a data-driven manner to infer the coefficients (α_i) have been proposed recently [30, 33]. The data-driven coefficients are particularly useful when the discretization in the n -point stencil is irregular and low-resolution where the fixed coefficients cause substantial numerical errors.

2.3 Time derivative module: PDE-specific module

Once upto d -order derivatives are modularized by learnable parameters, the modules are assembled by an additional module to learn the function $F(\cdot)$ in Eq. 2. This module is PDE-specific as the function F describes how the spatiotemporal observations change. The exact form of a ground truth PDE is not given. Instead, the time derivative module is data-driven and will be adapted to observations.

2.4 Modular meta-learning

As one branch of meta-learning, modular meta-learning [34] provides a good set of reusable modules from task-independent/-specific optimization to be quickly adapted to limited data. Suppose that $\mathcal{D} = (\mathcal{D}_1, \dots, \mathcal{D}_M)$ where $\mathcal{D}_i = (\mathcal{D}_i^{tr}, \mathcal{D}_i^{te})$ is a set of meta-learning datasets where M is the number of main tasks. There is a set of K -modules whose learnable parameters are $\Phi = (\phi_1, \dots, \phi_K)$ and the modules constitute a possible discrete structure $S \in \mathbb{S}$ where \mathbb{S} is a set of all possible discrete structures. The learning process of the structured modular meta-learning consists of two objectives for (1) task-specific adaptation (Eq. 4) and (2) updating module parameters (Eq. 5). The task-specific objective is used to find an adapted structure for a particular task i and the parameters in the modules are optimized by the accumulated loss across all tasks with learning rate α .

$$S_i = \arg \min_{S \in \mathbb{S}} \mathcal{L}(\mathcal{D}_i^{tr}, S, \Phi), \quad (4) \quad \Phi \leftarrow \Phi - \alpha \sum_i \nabla_{\Phi} \mathcal{L}(\mathcal{D}_i^{te}, S_i, \Phi). \quad (5)$$

Inspired by the success of modular meta-learning on combinatorial optimization and relational inference, we adjust the structured modular meta-learning to be adaptable to our PDE-independent/-specific modules for the spatiotemporal prediction task. As S_i is an adapted structure given a particular task i , the adaptation process corresponds to the optimization of the task-specific time derivative module. On the other hand, as Φ indicates generalizable task-independent knowledge, parameters of our PDE-independent spatial derivative modules can be regarded as meta-parameters.

3 Physics-aware modular meta-learning

In this section, we develop a physics-aware modular meta-learning method for the modularized PDEs and design neural network architectures for the modules. Fig. 1 describes the proposed framework and its computational process.

3.1 Spatial derivative module

As we focus on the modeling and prediction of sensor-based observations, where the available data points are inherently on a spatially sparse irregular grid, we use graph networks for each module ϕ_k to learn the finite difference coefficients [33]. Given a graph $\mathcal{G} = (\mathbb{V}, \mathbb{E})$ where $\mathbb{V} = \{1, \dots, N\}$ and $\mathbb{E} = \{(i, j) : i, j \in \mathbb{V}\}$, a node i denotes a physical location (x_i, y_i) where a function value is observed. The observation at node i is $u(x_i, y_i)$ or u_i . Then, the data-driven spatial derivatives are computed by Algorithm 1. Note that it is flexible to tune the number of hops in ϕ to increase/decrease

Algorithm 1 Spatial derivative module (SDM).

Input: Graph signals u and coordinates $\mathbf{x} = (x, y)$ on \mathcal{G} . A set of module attributes \mathbb{K}

Output: Approximated spatial derivatives $\{\hat{u}_{k,i} \mid i \in \mathbb{V} \text{ and } k \in \mathbb{K}\}$

Require: Randomly initialized spatial derivative modules $\{\phi_k \mid k \in \mathbb{K}\}$

```

1: for  $k \in \mathbb{K}$  do
2:    $\{a_{k,(i,j)}, b_{k,(i,j)} \mid (i,j) \in \mathbb{E} \text{ and } k \in \mathbb{K}\} = \phi_k(\{u\}, \{\mathbf{x}\}, \mathcal{G})$ 
3:   for  $i \in \mathbb{V}$  do
4:      $\hat{u}_{k,i} = \sum_{(i,j) \in \mathbb{E}} a_{k,(i,j)}(u_i - b_{k,(i,j)} \cdot u_j)$ 
5:   end for
6: end for

```

the kernel size, which corresponds to the size of stencil. The coefficients (a, b) on each edge (i, j) are output of ϕ and they are linearly combined with the function values on node i and j . \mathbb{K} denotes a set of finite difference operators. For example, if we set $\mathbb{K} = \{\nabla_x, \nabla_y, \nabla_x^2, \nabla_y^2\}$, we have 4 modules which approximate first/second order of spatial derivatives along the x and y direction, respectively.

3.2 Time derivative module

Once spatial derivatives are approximated, another learnable module is required to combine them for a target task. The form of line 2 in Algorithm 2 comes from Eq. 2 and TDM is adapted to learn $F(\cdot)$ in the equation. The exact form of F for the target task is not restricted. As our target task is the regression of graph signals, we use another graph network for TDM.

Algorithm 2 Time derivative module (TDM).

Input: Graph signals u and approximated spatial derivatives \hat{u}_k where $k \in \mathbb{K}$ on \mathcal{G} . Time interval Δt

Output: Prediction of signals at next time step $\hat{u}(t+1)$

Require: Randomly initialized TDM

```

1:  $\hat{u}_t = \text{TDM}(\{u_i, \hat{u}_{k,i} \mid i \in \mathbb{V} \text{ and } k \in \mathbb{K}\})$ 
2:  $\hat{u}(t+1) = u(t) + \hat{u}_t \cdot \Delta t$ 

```

3.3 Modular meta-learning with auxiliary objective

With these physics-aware modules, we propose a variant of the structured modular meta-learning framework [34, 35] for our task. While the structured modular meta-learning provides a good set of reusable modules optimized through meta-train tasks, its task-specific adaptation process is limited to the structural combination. The combinatorial searching for the task-specific adaptation has a couple of challenges. First, since an adapted structure comes from the pre-defined searching space, the set of possible structures (\mathbb{S}) should be large enough to make the optimal structure adaptable to unseen tasks. Second, a searching algorithm should be fast enough to handle a large number of modules. Finally, the role of each module is not specified as all modules are optimized by the common objective.

We generalize the adaptation process in the structured modular meta-learning as an optimization of the adaptation module to address the challenges. There are computational benefits to use the data-driven module instead of searching for an adapted structure. First, it has a continuous searching space and does not require a pre-defined searching space for possible structures. Second, the adaptation process is gradient-based so that it is not necessary to propose fast searching algorithms. Finally, since the module is learnable, it is easily adaptable to a new task without prior knowledge of the composition.

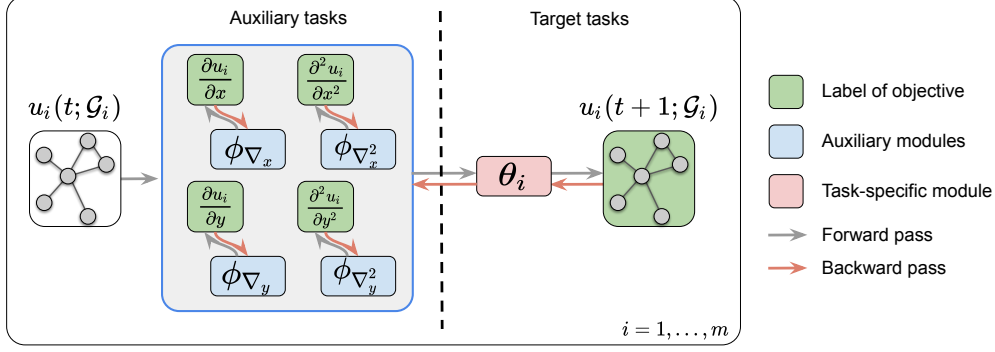


Figure 1: Schematic overview of the physics-aware modular meta-learning (PiMetal).

Algorithm 3 Proposed modular meta-learning with auxiliary tasks.

Input: A set of meta-train tasks $\mathcal{T} = \{\mathcal{T}_1, \dots, \mathcal{T}_M\}$ and task datasets $\mathcal{D} = \{\mathcal{D}_1, \dots, \mathcal{D}_M\}$ where $\mathcal{D}_i = (\mathcal{D}_i^{tr}, \mathcal{D}_i^{te})$. $\mathcal{D}_i = \{(\mathbf{x}_j^i, y_j^i, y_j^{(a_1, i)}, \dots, y_j^{(a_K, i)})\}_{j=1}^{N_i}$ where y_j^i is a main task label and $y_j^{(a_k, i)}$ is an k -th auxiliary task label of input \mathbf{x}_j^i , respectively. Learning rate α and β .

- 1: Initialize auxiliary modules $\Phi = (\phi_1, \dots, \phi_K)$ and task-specific modules $\Theta = (\theta_1, \dots, \theta_M)$
- 2: **while** not converged **do**
- 3: $\Delta = 0$
- 4: Sample batch of tasks $\{\mathcal{T}_1, \dots, \mathcal{T}_B\}$ from \mathcal{T}
- 5: **for** each task \mathcal{T}_i in $\{\mathcal{T}_1, \dots, \mathcal{T}_B\}$ **do**
- 6: $\theta_i \leftarrow \theta_i - \beta \nabla_{\theta_i} \mathcal{L}(\mathcal{D}_i^{tr}, \theta_i, \Phi)$
- 7: $\Delta \leftarrow \Delta + \nabla_{\Phi} \left(\mathcal{L}(\mathcal{D}_i^{te}, \theta_i, \Phi) + \sum_{j=1}^K \mathcal{L}_j(\mathcal{D}_i^{te}, \phi_j) \right)$
- 8: **end for**
- 9: $\Phi \leftarrow \Phi - \alpha \Delta$
- 10: **end while**

However, adding the learnable module for the task adaptation causes the task-independent modules to lose module-specific representation since the parameters in the modules are exclusively updated by the main task. We introduce auxiliary tasks for optimizing the task-independent modules to mitigate the shift. Each auxiliary task provides a set of input/output pairs to explicitly impose the desired function to each module. Algorithm 3 shows how the auxiliary tasks are introduced in the modular meta-learning. For PDEs, we propose physics-aware modular meta-learning with auxiliary tasks (**PiMetal-modular**) and the auxiliary tasks are regression tasks of spatial derivatives (e.g., $\partial u_i / \partial x$ is used to regularize the ϕ_x module in Fig. 1).

The procedure departs from the structured modular meta-learning (Eq. 4 and 5) in two aspects: (1) the adaptation to a specific task (\mathcal{T}_i) is parameterized by a learnable module θ_i (line 6) and (2) the auxiliary objective is added (line 7) for optimizing auxiliary modules. The auxiliary modules (Φ) are updated by two loss functions: a task-specific and a sum of task-independent loss functions. The former makes the module flexible to different tasks as meta-initialization [14] does and the latter one imposes the auxiliary module to learn an auxiliary task.

Variation of updating rule (PiMetal-MAML) Many gradient-based algorithms can be easily applied with the two objectives in Algorithm 3. For example, we use MAML by replacing line 6 in Algorithm 3 by Eq. 6. Then, Φ and θ_i will be updated by the accumulated losses (Eq. 7), respectively.

$$\theta'_i \leftarrow \theta_i - \beta \nabla_{\theta_i} \mathcal{L}(\mathcal{D}_i^{tr}, \theta_i, \Phi), \quad \Phi' \leftarrow \Phi - \beta \nabla_{\Phi} \mathcal{L}(\mathcal{D}_i^{tr}, \theta_i, \Phi), \quad (6)$$

$$\theta_i \leftarrow \theta_i - \alpha \nabla_{\theta_i} \mathcal{L}(\mathcal{D}_i^{te}, \theta'_i, \Phi'), \quad \Delta \leftarrow \Delta + \nabla_{\Phi} \left(\mathcal{L}(\mathcal{D}_i^{te}, \theta'_i, \Phi') + \sum_{j=1}^K \mathcal{L}_j(\mathcal{D}_i^{te}, \phi'_j) \right). \quad (7)$$

Table 1: Description of the sizes of all datasets.

	Meta-train		Meta-test		
	Synthetic	Synthetic	AQI-CO [7]	ExtremeWeather [8]	NOAA
Number of nodes (N)	246	[150,400]	[51,58]	[39,214]	191
Length of sequences (T)	20	20	24	20	[13,24]
Number of tasks (M)	100	10	12	10	12

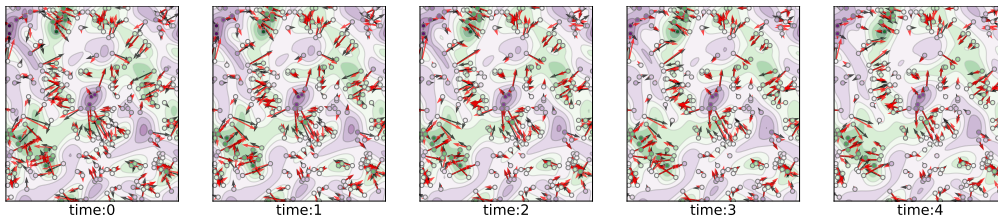


Figure 2: Spatiotemporal dynamics from the convection-diffusion equation. Dots represent the sampled points. Black arrows represent the first-order derivative at each point, and red arrows show the prediction of the first-order derivatives from the spatial derivative module.

4 Experimental evaluation

Overview of the evaluations: We adopt a set of multi-step spatiotemporal sequence prediction tasks to evaluate our proposed framework. In each task, the data is a sequence of T frames, where each frame is a set of observations on N nodes in space, and we train an auto-regressive model with the first k frames (k -shot) and evaluate its performance with the following $T - k$ frames. We evaluate the performance of the model via the average of mean squared errors (MSEs) over all tasks.

For all experiments, we generate meta-train tasks from the 2D convection-diffusion equation (Eq. 8) as all target quantities have fluidic properties such as diffusive and convection. Fig. 2 shows the spatiotemporal dynamics from the meta-train data and the prediction of 1st-order spatial derivatives from the spatial derivative module, which is close to the ground truth spatial derivatives.

We choose different datasets for meta-test tasks. Table 1 shows the sizes of all datasets and more details are in the supplementary material.

PiMetaL variants and baselines:

We evaluate the performance of (1) a Recurrent Graph Neural Network architecture (RGN) [36] and (2) a physics-aware architecture (PA-DGN) [33] with spatial derivative modules (SDM) and temporal derivative modules (TDM), where the SDM is a Graph Neural Network and the TDM is a Recurrent Graph Neural Network. For the RGN architecture, we evaluate its performance via (1)

training on meta-test tasks only (**train from scratch**), (2) training on meta-train tasks and using the trained model weights for the initialization of models trained on meta-test tasks (**weight init**), (3) model-agnostic meta training (MAML) [14]. For the PA-DGN architecture, in addition to train from scratch and weight init, we consider 2 versions of our proposed physics-aware modular meta-learning methods: (1) the vanilla modular meta-learning with auxiliary tasks in Algorithm 3 (**PiMetaL-modular**) and (2) the MAML variation in Eq. 6 and 7 (**PiMetaL-MAML**). Details of architectures and implementation of models are in the supplementary material.

Table 2: Multi-step prediction results of the synthetic dataset.

Method	5-shot	10-shot
RGN (train from scratch)	1.305E+00	4.608E-01
PA-DGN (train from scratch)	1.589E+00	4.598E-01
RGN (weight init)	1.123E+00	4.461E-01
PA-DGN (weight init)	1.443E+00	3.464E-01
RGN (MAML)	1.127E+00	4.467E-01
PiMetaL-modular	1.278E+00	3.017E-01
PiMetaL-MAML	8.326E-01	2.952E-01

4.1 Synthetic data

Data generation: We evaluate our proposed framework with the synthetic dataset sampled from the solution of the following convection-diffusion equation:

$$\begin{aligned} \dot{u}_i(t) &= \mathbf{v}_i \cdot \nabla u_i(t) + c_i \nabla^2 u_i(t), \quad i = 1, 2, \dots, N \\ u_i(0) &= \sum_{|k|, |l| \leq F} \lambda_{k,l} \cos(kx_i + ly_i) + \gamma_{k,l} \sin(kx_i + ly_i), \quad F = 9, \lambda_{k,l}, \gamma_{k,l} \sim \mathcal{N}(0, 0.02), \end{aligned} \quad (8)$$

where the index i denotes the i -th node whose coordinate is (x_i, y_i) in the 2D space $([0, 2\pi] \times [0, 2\pi])$ and $\mathbf{v}_i = (a_i, b_i)$ is velocity field such that $a_i = 0.5\lambda(\cos(y_i) + x_i(2\pi - x_i)\sin(x_i)) + 0.6$, $b_i = 2\lambda(\cos(y_i) + \sin(x_i)) + 0.8$, and $c_i = D$. k, l are randomly sampled integers. λ, D are hyper-parameters to control the data distribution. We set $\lambda = 1, D = 0.2$ for meta-train tasks and $\lambda = 0.8, D = 0.1$ for meta-test tasks. From the synthetic data, we compute the first-order and the second-order derivatives and use the regression tasks on them as the auxiliary tasks (See Fig. 1).

Discussion: Table 2 shows the multi-step prediction performance of all methods on the 2D convection-diffusion dataset. In both 5-shot and 10-shot settings, our proposed framework (PiMetaL-MAML) has the lowest multi-step prediction error. Fig. 3 shows test error curves of all methods on one task during the meta-test stage. While other methods quickly over-fit due to the limited amount of training data, PiMetaL-MAML is resistant to over-fitting and has the smallest test error.

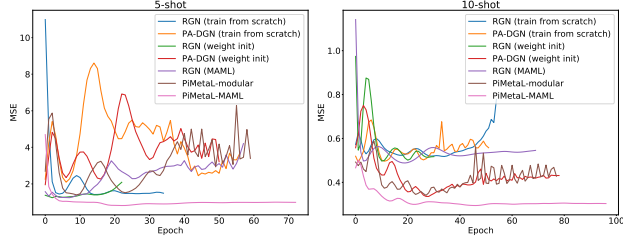


Figure 3: 5-shot/10-shot test error curves.

4.2 Real-world data experiments

4.2.1 Real-world data: single feature, multi-step prediction

Datasets: We evaluate our proposed framework with 2 real-world datasets: (1) **AQI-CO**: national air quality index (AQI) observations [7]; (2) **ExtremeWeather**: the extreme weather dataset [8]. For the AQI-CO dataset, we construct 12 meta-test tasks with the carbon monoxide (CO) ppm records from the first week of each month in 2015 at land-based stations. For the ExtremeWeather dataset, we select the top-10 extreme weather events with the longest lasting time from the year 1984 and construct a meta-test task from each event with the observed surface temperatures at randomly sampled locations. Since each event lasts fewer than 20 frames, each task has a very limited amount of available data. In both datasets, only one time-varying feature is available.

Discussion: Table 3 shows the multi-step prediction performance of our proposed framework against the baselines in Sec. 4.1 on real-world datasets.

On the AQI-CO dataset, our framework (PiMetaL-modular) outperforms all other baselines in the multi-step prediction task under both 5-shot and 10-shot settings. The variant of our proposed framework (PiMetaL-MAML) has the lowest multi-step prediction error on the ExtremeWeather dataset under the 5-shot setting. Although RGN methods have lower prediction error for the 10-shot setting, evaluations in Sec. 4.2.2 show that our method can still handle datasets with multiple features even when the meta-train data has only one single feature, where RGN-based methods are not applicable.

Table 3: Multi-step prediction results of datasets (single feature).

	Method	AQI-CO	ExtremeWeather
5-shot	RGN (train from scratch)	8.429E-02	5.658E-01
	PA-DGN (train from scratch)	2.848E-02	1.050E+00
	RGN (weight init)	9.332E-02	5.910E-01
	PA-DGN (weight init)	1.841E-01	9.679E-01
	RGN (MAML)	7.904E-02	6.194E-01
	PiMetaL-modular	1.630E-02	9.390E-01
	PiMetaL-MAML	1.025E-01	4.959E-01
10-shot	RGN (train from scratch)	5.821E-02	4.177E-01
	PA-DGN (train from scratch)	1.454E-02	4.271E-01
	RGN (weight init)	5.819E-02	3.294E-01
	PA-DGN (weight init)	1.123E-02	4.111E-01
	RGN (MAML)	5.578E-02	3.607E-01
	PiMetaL-modular	1.079E-02	4.081E-01
	PiMetaL-MAML	7.445E-02	3.859E-01

4.2.2 Real-world data: multiple feature, multi-step prediction

One advantage of our framework is that the spatial derivative modules can be combined with PDE-specific modules with different architectures from the ones used in the meta-train stage, which enables our proposed framework to apply to tasks requiring multiple features that cannot be generated in synthetic data. Here we show its performance as an example on the task of (1) **ExtremeWeather**:

predicting surface temperature at randomly sampled locations in an extreme weather process and (2) **NOAA**: predicting temperature observations from the land-based weather stations recorded in the National Oceanic and Atmospheric Administration (NOAA) database [33]. Both tasks have features in addition to the prediction target, which cannot be generated in synthetic datasets.

Discussion: Table 4 shows the prediction performance of our proposed framework on two datasets that contain multiple features not in the meta-train tasks, and thus the PDE-specific part of the prediction model does not share the same architecture used for

Table 4: Multi-step prediction results on datasets with multiple features.

	Method	ExtremeWeather	NOAA
5-shot	PA-DGN (train from scratch)	8.344E-01	7.114E-01
	PA-DGN (weight init)	8.266E-01	7.151E-01
	PiMetaL-modular	8.114E-01	5.014E-01
10-shot	PA-DGN (train from scratch)	4.232E-01	6.560E-01
	PA-DGN (weight init)	4.235E-01	6.311E-01
	PiMetaL-modular	4.212E-01	6.207E-01

meta-train. As a result, task-specific RGN models are not applicable. On the contrary, our proposed framework enables the reuse of the spatial derivative module meta-trained with auxiliary tasks, and still outperforms other baselines when combining it with a task-specific temporal derivative module with a different architecture.

5 Related work

Physics-informed learning Since physics-informed neural networks are introduced [37] which find that a solution of a PDE can be discovered by neural networks, physical knowledge has been used as an inductive bias for deep neural networks. Advection-diffusion equation is incorporated with deep neural networks for sea-surface temperature dynamics [27]. [28, 29] show that Lagrangian/Hamiltonian mechanics can be imposed to learn the equations of motion of a mechanical system and [38] regularizes a graph neural network with a specific physics equation. Rather than using explicitly given equations, physics-inspired inductive bias is also used for reasoning dynamics of discrete objects [39, 40] and continuous quantities [33]. While there are many physics-involved works, to the best of our knowledge, we are the first to provide a framework to use the physics-inspired inductive bias under the meta-learning settings to tackle the limited data issue which is pretty common for real-world data such as extreme weather events [8].

Meta-learning The aim of meta-learning is to enable learning parameters which can be used for new tasks unknown at the time of learning, leading to agile models which adapt to a new task utilizing only a few samples [11, 41, 42]. Based on how the knowledge from the related tasks is used, meta-learning methods have been classified as optimization-based [12, 43, 44, 14, 45, 46, 47, 48], model-based [13, 49, 44, 50], and metric-based [51, 52, 53]. Recently, another branch of meta-learning has been introduced to more focus on finding a set of reusable modules as components of a solution to a new task. [34, 35] provide a framework, structured modular meta-learning, where a finite number of modules are introduced as task-independent modules and an optimal structure combining the modules is found from a limited number of data. [54] introduces techniques to automatically discover task-independent/dependent modules based on Bayesian shrinkage to find which modules are more adaptable. To our knowledge, none of the above works provide a solution to use meta-learning for modeling physics-related spatiotemporal dynamics.

6 Conclusion

In this paper, we propose a framework for physics-aware modular meta-learning with auxiliary tasks. By incorporating PDE-independent knowledge from simulated data, the framework rapidly adapts to meta-test tasks with a limited amount of available data. Experiments show that auxiliary tasks and physics-aware modular meta-learning help construct reusable modules that improve the performance of spatiotemporal predictions in real-world tasks where data is limited. Although introducing auxiliary tasks based on synthetic datasets improves the prediction performance, they need to be chosen and constructed manually and intuitively. Designing and identifying the most useful auxiliary tasks and data will be the focus of our future work.

References

- [1] A Manepalli, A Albert, A Rhoades, D Feldman, and M Prabhat. Emulating numeric hydroclimate models with physics-informed conditional generative adversarial networks. *Environmetrics*, 2019.
- [2] Ján Drgona, Lieve Helsen, and Draguna Vrabie. Stripping off the implementation complexity of physics-based model predictive control for buildings via deep learning. <https://www.nips.cc/>, 2019.
- [3] Gautier Cosne, Guillaume Maze, and Pierre Tandeo. Coupling oceanic observation systems to study mesoscale ocean dynamics. *arXiv preprint arXiv:1910.08573*, 2019.
- [4] Ping-Wei Soh, Jia-Wei Chang, and Jen-Wei Huang. Adaptive deep learning-based air quality prediction model using the most relevant spatial-temporal relations. *Ieee Access*, 6:38186–38199, 2018.
- [5] Shengdong Du, Tianrui Li, Yan Yang, and Shi-Jinn Horng. Deep air quality forecasting using hybrid deep learning framework. *arXiv preprint arXiv:1812.04783*, 2018.
- [6] Yijun Lin, Nikhit Mago, Yu Gao, Yaguang Li, Yao-Yi Chiang, Cyrus Shahabi, and José Luis Ambite. Exploiting spatiotemporal patterns for accurate air quality forecasting using deep learning. In *Proceedings of the 26th ACM SIGSPATIAL International Conference on Advances in Geographic Information Systems*, pages 359–368, 2018.
- [7] Lex Berman. National AQI Observations (2014-05 to 2016-12), 2017.
- [8] Evan Racah, Christopher Beckham, Tegan Maharaj, Samira Ebrahimi Kahou, Mr Prabhat, and Chris Pal. Extremeweather: A large-scale climate dataset for semi-supervised detection, localization, and understanding of extreme weather events. In *Advances in Neural Information Processing Systems*, pages 3402–3413, 2017.
- [9] Wei Cao, Dong Wang, Jian Li, Hao Zhou, Lei Li, and Yitan Li. Brits: Bidirectional recurrent imputation for time series. In *Advances in Neural Information Processing Systems*, pages 6775–6785, 2018.
- [10] Xianfeng Tang, Huaxiu Yao, Yiwei Sun, Charu Aggarwal, Prasenjit Mitra, and Suhang Wang. Joint modeling of local and global temporal dynamics for multivariate time series forecasting with missing values. *arXiv preprint arXiv:1911.10273*, 2019.
- [11] Jürgen Schmidhuber. *Evolutionary principles in self-referential learning, or on learning how to learn: The meta-meta-... hook*. Diplomarbeit, Technische Universität München, München, 1987.
- [12] Marcin Andrychowicz, Misha Denil, Sergio Gomez, Matthew W Hoffman, David Pfau, Tom Schaul, Brendan Shillingford, and Nando De Freitas. Learning to learn by gradient descent by gradient descent. In *Advances in neural information processing systems*, pages 3981–3989, 2016.
- [13] Adam Santoro, Sergey Bartunov, Matthew Botvinick, Daan Wierstra, and Timothy Lillicrap. Meta-learning with memory-augmented neural networks. In *Proceedings of The 33rd International Conference on Machine Learning*, pages 1842–1850, 2016.
- [14] Chelsea Finn, Pieter Abbeel, and Sergey Levine. Model-agnostic meta-learning for fast adaptation of deep networks. In *Proceedings of the 34th International Conference on Machine Learning-Volume 70*, pages 1126–1135. JMLR. org, 2017.
- [15] Sinno Jialin Pan and Qiang Yang. A survey on transfer learning. *IEEE Transactions on knowledge and data engineering*, 22(10):1345–1359, 2009.
- [16] Sinno Jialin Pan, Ivor W Tsang, James T Kwok, and Qiang Yang. Domain adaptation via transfer component analysis. *IEEE Transactions on Neural Networks*, 22(2):199–210, 2010.
- [17] Yaroslav Ganin and Victor Lempitsky. Unsupervised domain adaptation by backpropagation. *arXiv preprint arXiv:1409.7495*, 2014.
- [18] David Lopez-Paz and Marc’Aurelio Ranzato. Gradient episodic memory for continual learning. In *Advances in Neural Information Processing Systems*, pages 6467–6476, 2017.
- [19] Aniruddh Raghu, Maithra Raghu, Samy Bengio, and Oriol Vinyals. Rapid learning or feature reuse? towards understanding the effectiveness of maml. *arXiv preprint arXiv:1909.09157*, 2019.

- [20] Kaiming He, Georgia Gkioxari, Piotr Dollár, and Ross Girshick. Mask r-cnn. In *Proceedings of the IEEE international conference on computer vision*, pages 2961–2969, 2017.
- [21] Jacob Andreas, Marcus Rohrbach, Trevor Darrell, and Dan Klein. Neural module networks. In *Proceedings of the IEEE Conference on Computer Vision and Pattern Recognition*, pages 39–48, 2016.
- [22] Akira Fukui, Dong Huk Park, Daylen Yang, Anna Rohrbach, Trevor Darrell, and Marcus Rohrbach. Multimodal compact bilinear pooling for visual question answering and visual grounding. *arXiv preprint arXiv:1606.01847*, 2016.
- [23] Jia Deng, Wei Dong, Richard Socher, Li-Jia Li, Kai Li, and Li Fei-Fei. Imagenet: A large-scale hierarchical image database. In *2009 IEEE conference on computer vision and pattern recognition*, pages 248–255. Ieee, 2009.
- [24] Karen Simonyan and Andrew Zisserman. Very deep convolutional networks for large-scale image recognition. *arXiv preprint arXiv:1409.1556*, 2014.
- [25] Kaiming He, Xiangyu Zhang, Shaoqing Ren, and Jian Sun. Deep residual learning for image recognition. In *Proceedings of the IEEE conference on computer vision and pattern recognition*, pages 770–778, 2016.
- [26] Mark Sandler, Andrew Howard, Menglong Zhu, Andrey Zhmoginov, and Liang-Chieh Chen. Mobilenetv2: Inverted residuals and linear bottlenecks. In *Proceedings of the IEEE conference on computer vision and pattern recognition*, pages 4510–4520, 2018.
- [27] Emmanuel de Bezenac, Arthur Pajot, and Patrick Gallinari. Deep learning for physical processes: Incorporating prior scientific knowledge. In *International Conference on Learning Representations*, 2018.
- [28] Michael Lutter, Christian Ritter, and Jan Peters. Deep lagrangian networks: Using physics as model prior for deep learning. *arXiv preprint arXiv:1907.04490*, 2019.
- [29] Samuel Greydanus, Misko Dzamba, and Jason Yosinski. Hamiltonian neural networks. In *Advances in Neural Information Processing Systems*, pages 15353–15363, 2019.
- [30] Yohai Bar-Sinai, Stephan Hoyer, Jason Hickey, and Michael P Brenner. Learning data-driven discretizations for partial differential equations. *Proceedings of the National Academy of Sciences*, 116(31):15344–15349, 2019.
- [31] Jiawei Zhuang, Dmitrii Kochkov, Yohai Bar-Sinai, Michael P Brenner, and Stephan Hoyer. Learned discretizations for passive scalar advection in a 2-d turbulent flow. *arXiv preprint arXiv:2004.05477*, 2020.
- [32] Tian Qi Chen, Yulia Rubanova, Jesse Bettencourt, and David K Duvenaud. Neural ordinary differential equations. In *Advances in neural information processing systems*, pages 6571–6583, 2018.
- [33] Sungyong Seo, Chuizheng Meng, and Yan Liu. Physics-aware difference graph networks for sparsely-observed dynamics. In *International Conference on Learning Representations*, 2020.
- [34] Ferran Alet, Tomás Lozano-Pérez, and Leslie P Kaelbling. Modular meta-learning. *arXiv preprint arXiv:1806.10166*, 2018.
- [35] Ferran Alet, Erica Weng, Tomás Lozano-Pérez, and Leslie Pack Kaelbling. Neural relational inference with fast modular meta-learning. In *Advances in Neural Information Processing Systems*, pages 11804–11815, 2019.
- [36] Peter W Battaglia, Jessica B Hamrick, Victor Bapst, Alvaro Sanchez-Gonzalez, Vinicius Zambaldi, Mateusz Malinowski, Andrea Tacchetti, David Raposo, Adam Santoro, Ryan Faulkner, et al. Relational inductive biases, deep learning, and graph networks. *arXiv preprint arXiv:1806.01261*, 2018.
- [37] Maziar Raissi, Paris Perdikaris, and George E Karniadakis. Physics-informed neural networks: A deep learning framework for solving forward and inverse problems involving nonlinear partial differential equations. *Journal of Computational Physics*, 378:686–707, 2019.
- [38] Sungyong Seo and Yan Liu. Differentiable physics-informed graph networks. *arXiv preprint arXiv:1902.02950*, 2019.

- [39] Peter Battaglia, Razvan Pascanu, Matthew Lai, Danilo Jimenez Rezende, et al. Interaction networks for learning about objects, relations and physics. In *Advances in neural information processing systems*, pages 4502–4510, 2016.
- [40] Michael B Chang, Tomer Ullman, Antonio Torralba, and Joshua B Tenenbaum. A compositional object-based approach to learning physical dynamics. *arXiv preprint arXiv:1612.00341*, 2016.
- [41] Devang K Naik and Richard J Mammone. Meta-neural networks that learn by learning. In *[Proceedings 1992] IJCNN International Joint Conference on Neural Networks*, volume 1, pages 437–442. IEEE, 1992.
- [42] Sebastian Thrun and Lorien Pratt. Learning to learn: Introduction and overview. In *Learning to learn*, pages 3–17. Springer, 1998.
- [43] Sachin Ravi and Hugo Larochelle. Optimization as a model for few-shot learning. In *International Conference on Learning Representations*, 2017.
- [44] Yan Duan, Marcin Andrychowicz, Bradly Stadie, OpenAI Jonathan Ho, Jonas Schneider, Ilya Sutskever, Pieter Abbeel, and Wojciech Zaremba. One-shot imitation learning. In *Advances in neural information processing systems*, pages 1087–1098, 2017.
- [45] Alex Nichol, Joshua Achiam, and John Schulman. On first-order meta-learning algorithms. *arXiv preprint arXiv:1803.02999*, 2018.
- [46] Antreas Antoniou, Harrison Edwards, and Amos Storkey. How to train your maml. *arXiv preprint arXiv:1810.09502*, 2018.
- [47] Andrei A Rusu, Dushyant Rao, Jakub Sygnowski, Oriol Vinyals, Razvan Pascanu, Simon Osindero, and Raia Hadsell. Meta-learning with latent embedding optimization. *arXiv preprint arXiv:1807.05960*, 2018.
- [48] Erin Grant, Chelsea Finn, Sergey Levine, Trevor Darrell, and Thomas Griffiths. Recasting gradient-based meta-learning as hierarchical bayes. *arXiv preprint arXiv:1801.08930*, 2018.
- [49] Tsendsuren Munkhdalai and Hong Yu. Meta networks. In *Proceedings of the 34th International Conference on Machine Learning-Volume 70*, pages 2554–2563. JMLR. org, 2017.
- [50] Nikhil Mishra, Mostafa Rohaninejad, Xi Chen, and Pieter Abbeel. A simple neural attentive meta-learner. In *International Conference on Learning Representations*, 2018.
- [51] Gregory Koch, Richard Zemel, and Ruslan Salakhutdinov. Siamese neural networks for one-shot image recognition. In *ICML deep learning workshop*, volume 2. Lille, 2015.
- [52] Oriol Vinyals, Charles Blundell, Timothy Lillicrap, Daan Wierstra, et al. Matching networks for one shot learning. In *Advances in neural information processing systems*, pages 3630–3638, 2016.
- [53] Jake Snell, Kevin Swersky, and Richard Zemel. Prototypical networks for few-shot learning. In *Advances in neural information processing systems*, pages 4077–4087, 2017.
- [54] Yutian Chen, Abram L Friesen, Feryal Behbahani, David Budden, Matthew W Hoffman, Arnaud Doucet, and Nando de Freitas. Modular meta-learning with shrinkage. *arXiv preprint arXiv:1909.05557*, 2019.
- [55] Evan Racah, Christopher Beckham, Tegan Maharaj, Samira Kahou, Mr. Prabhat, and Chris Pal. Extremeweather: A large-scale climate dataset for semi-supervised detection, localization, and understanding of extreme weather events. In I. Guyon, U. V. Luxburg, S. Bengio, H. Wallach, R. Fergus, S. Vishwanathan, and R. Garnett, editors, *Advances in Neural Information Processing Systems 30*, pages 3405–3416. Curran Associates, Inc., 2017.

Supplementary Materials

A Datasets and tasks

A.1 Meta-train

Data: For all experiments, we generate the data of meta-train tasks from the 2D convection-diffusion equation (Eq. 8). We set $\lambda = 1$, $D = 0.2$ for meta-train data.

We first solve the equation on a 100×100 grid with the spectral method under the time resolution $5e-3$, then uniformly sample 250 locations from all grid points as observed nodes to simulate the case where the observations are irregularly distributed in space. We then construct a 4-Nearest Neighbor (NN) graph based on the Euclidean distance as the input of Graph Neural Networks.

Tasks: We construct 100 sequences, each with the initial condition generated from Eq. 8 using a unique random seed. Each sequence lasts 20 frames with the timestep size 0.01. We set up 1 k -shot meta-train task on each sequence: predicting the values and 1st/2nd-order spatial derivatives on all nodes for all frames with an auto-regressive model given the first frame as the input. The first k frames are used for training and the rest $20 - k$ frames for test. We select $k = 5, 10$ as two experiment settings.

A.2 Meta-test

A.2.1 Synthetic

Data: We generate the synthetic meta-test data from Eq. 8 but set $\lambda = 0.8$, $D = 0.1$ to simulate the realistic scenario where meta-train tasks and meta-test tasks do not share the same distribution.

Tasks: We reuse the method in A.1 to generate data and construct 10 meta-test tasks for the synthetic meta-test experiment.

A.2.2 Real-world, single feature

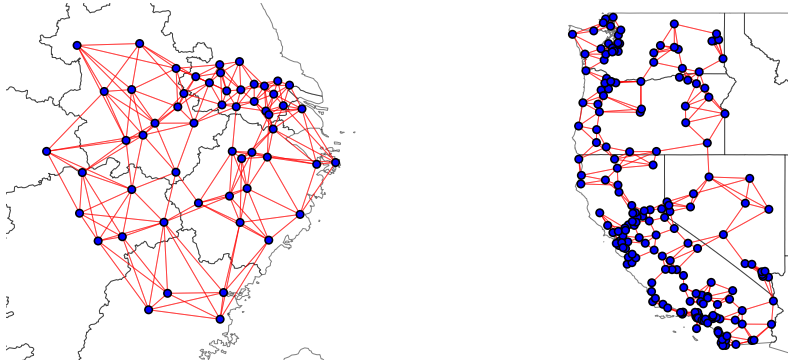


Figure A1: (Left) sensor locations in the AQI-CO dataset. (Right) weather station locations in the NOAA dataset. We show sensors/stations as blue nodes and edges of k -NN graphs as red lines. Borders of provinces/states are shown in grey.

Data:

- **AQI-CO [7]:** There are multiple pollutants in the dataset and we choose carbon monoxide (CO) ppm as a target pollutant in this paper. We select sensors located in between latitude (26, 33) and longitude (115,125) (East region of China). In this region, we sample multiple multivariate time series whose length should be larger than 12 steps (12 hours) for multiple meta-tasks. There are around 60 working sensors and the exact number of the working sensors is varying over different tasks. Fig. A1 (left) shows the locations of selected AQI sensors.

- **ExtremeWeather:** We select the data in the year 1984 from the extreme weather dataset in [55]. The data is an array of shape (1460, 16, 768, 1152), containing 1460 frames (4 per day, 365 days in the year). 16 channels in each frame correspond to 16 spatiotemporal variables. Each channel has a size of 768×1152 corresponding to one measurement per 25 square km on earth. For each frame, the dataset provides fewer than or equal to 15 bounding boxes, each of which labels the region affected by an extreme weather event and one of the four types of the extreme weather: (1) tropical depression, (2) tropical cyclone, (3) extratropical cyclone, (4) atmospheric river. In the single feature setting, we only utilize the channel of surface temperature (TS).

Tasks:

- **AQI-CO:** We select the first sequence of carbon monoxide (CO) ppm records from each month in the year 2015 at land-based stations, and set up the meta-test task on each sequence as the prediction of CO ppm. We construct a 6-NN graph based on the geodesic distances among stations.
- **ExtremeWeather:** First, we aggregate all bounding boxes into multiple sequences. In each sequence, all bounding boxes (1) are in consecutive time steps, (2) are affected by the same type of extreme weather, and (3) have an intersection over union (IoU) ratio above 0.25 with the first bounding box in the sequence. Then we select the top-10 longest sequences. For each sequence, we consider its first bounding box A as the region affected by an extreme weather event, and extend it to a new sequence of 20 frames by cropping and appending the same region A from successive frames. For each region we uniformly sample 10% of available pixels as observed nodes to simulate irregularly spaced weather stations and build a 4-NN graph based on the Euclidean distance. Fig. A2 visualizes the first 5 frames of one extended sequence. In the single feature experiment, we set up a meta-test task on each extended sequence as the prediction of the surface temperature (TS) on all observed nodes with the initial TS given only.

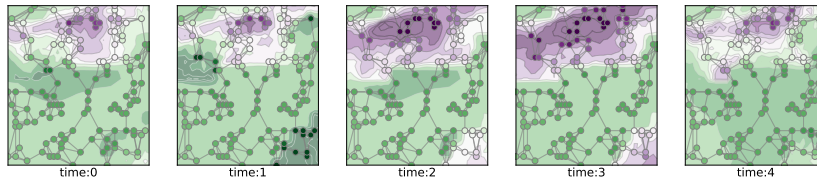


Figure A2: Visualization of the first 5 frames of one extended sequence in the ExtremeWeather dataset. Dots represent the sampled points. Area with high surface temperature (TS) are colored with green and area with low TS are colored with purple.

A.2.3 Real-world, multiple features

Data:

- **ExtremeWeather:** We use the same ExtremeWeather dataset as in A.2.2. In the multiple features setting, we consider all channels as input features but still predict the surface temperature (TS) only.
- **NOAA:** We select the consecutive observations in the year 2015 of weather stations located in 4 west states (Washington, Oregon, California and Nevada) from the Online Climate Data Directory of the National Oceanic and Atmospheric Administration (NOAA). Locations of stations are shown in Fig. A1 (right). The time interval between 2 consecutive frames is 1 hour. We construct a 4-NN graph based on the geodesic distances among weather stations. In the multiple features setting, we use the temperature and the altitude of the station as input features to forecast the temperature.

Tasks:

- **ExtremeWeather:** We construct meta-test tasks with the method in A.2.2. In the multiple features setting, the meta-test task is still the prediction of TS. All other 15 features (channels)

are fully observed on all nodes during the whole prediction process, but TS is only available in the initial frame.

- **NOAA**: We select the longest consecutive sequence from each month in the year 2015, and set up a temperature prediction task as the meta-test task on each sequence.

B Experimental details

B.1 Model Architectures

- **RGN [36]**: A recurrent graph neural network model with 2 GN blocks. Each GN block has an edge update block and a node update block, both of which use a 2-layer GRU cell as the update function. We set its hidden dimension to 73. The RGN model has 394526 learnable parameters.
- **PA-DGN [33]**: The spatial derivative layer uses a message passing neural network (MPNN) with 2 GN blocks using 2-layer MLPs as update functions. The forward network part uses a recurrent graph neural network with 2 recurrent GN blocks using 2-layer GRU cells as update functions. We set its hidden dimension to 64, in which case PA-DGN has a similar number of parameters with RGN. The PA-DGN model has 384653 learnable parameters.

B.2 Baselines

- **RGN (train from scratch)**: For each meta-test task, initialize one RGN model randomly and train it on the single task.
- **PA-DGN (train from scratch)**: For each meta-test task, initialize one PA-DGN model randomly and train it on the single task.
- **RGN (weight init)**: First pre-train one RGN model on all meta-train tasks with the sequence prediction loss. Then for each meta-test task, initialize one RGN model with the weights from the pre-training stage and train it on the single task.
- **PA-DGN (weight init)**: First pre-train one PA-DGN model on all meta-train tasks with both the sequence prediction loss and the auxiliary loss (loss on spatial derivatives). Then for each meta-test task, initialize one PA-DGN model with the weights from the pre-training stage and train it on the single task.
- **RGN (MAML)**: Meta-train one RGN model on all meta-train tasks with model-agnostic meta-learning (MAML) [14] with the sequence prediction loss. Then for each meta-test task, initialize one RGN model with the weights from the meta-training stage and train it on the single task.

B.3 Ours

- **PiMetaL-modular**: Meta-train one PA-DGN model with our proposed Algorithm 3. Then for each meta-test task, initialize one PA-DGN model with the weights from the pre-training stage and train it on the single task.
- **PiMetaL-MAML**: Meta-train one PA-DGN model with the MAML variant of Algorithm 3 (Eq. 6 and Eq. 7). Then for each meta-test task, initialize one PA-DGN model with the weights from the pre-training stage and train it on the single task.

B.4 Training settings

Training hyperparameters: For all meta-train and meta-test tasks, we use the Adam optimizer with the learning rate $1e-3$. In each training epoch, we sample 1 task from all available tasks.

Environments: All experiments are implemented with Python3.6 and PyTorch 1.3.0, and are conducted with NVIDIA GTX 1080 Ti GPUs.

Runtime: The baselines RGN (train from scratch) and PA-DGN (train from scratch) will finish in 30 minutes. All other baselines will finish the meta-train stage in 4 hours and the meta-test stage in 2 hours. The runtime is measured in environments described above.